Key Engineering Materials
ISSN: 1662-9795, Vol. 926, pp 1907-1913
doi:10.4028/p-7zs542

Submitted: 2021-12-07
Revised: 2022-01-28
Accepted: 2022-02-04
Online: 2022-07-22

Measurement of Biaxial Deformation Behavior and Material Modeling for HI-PVC Using Multiaxial Tube Expansion Test

Shintaro Obuchi[1,a], Sohta Kubo[1,b] and Toshihiko Kuwabara[1,c*], etc.

[1]Tokyo University Agriculture and Technology, Japan

[a]obuchi@st.go.tuat.ac.jp; [b]s200945s@st.go.tuat.ac.jp; [c]kuwabara@cc.tuat.ac.jp

Keywords: High Impact Polyvinyl Chloride, Multiaxial tube expansion test, Material modeling

Abstract. This study investigates the biaxial deformation behavior of the High Impact Polyvinyl Chloride (HI-PVC) used as a water pipe material. Multiaxial tube expansion test (MTET) was performed on the HI-PVC circular tube, and the stress-strain curves were measured for nine linear stress paths. The contours of plastic work and the directions of the plastic strain rates were also measurd. The experimental results show that the test sample has strong anisotropy. Anisotropic hardening behavior was also confirmed from the evolution of the work contours. It was confirmed that the Yld2000-2d yield function had a better agreement with the measued work contour than Hill's quadratic and the von Mises yield functons. Moreover, it was found that the test sample follows the normality rule with the Yld2000-2d yield function.

Introduction

Resin materials are widely used as general-purpose materials because of their ease of molding. With the advent of engineering plastics that exhibit excellent durability, they are widely applied to structural materials from urban infrastructure, such as water pipes, to the automobile industry [1]. Polyvinyl Chloride (PVC) is cheaper than other resin materials and has excellent corrosion resistance, so it has been rapidly laid as a water pipe from high economic miracle period [2]. In recent years, however, the number of water pipes that reach the end of their useful life is increasing rapidly, and the aging of PVC pipes has become a serious problem [3]. In addition, the 2011 Great East Japan Earthquake and the 2016 Kumamoto Earthquake caused enormous damage to water pipes; therefore, water pipes with excellent earthquake resistance are required. However, among the basic water pipes, those with earthquake resistance remained at about 39.3% at the end of 2017. Therefore, it is necessary to urgently proceed with measures against aging and replacement with earthquake-resistant water pipes.

The shift to High Impact PVC (HI-PVC), which has better impact resistance than PVC, is progressing, but the mechanical material property evaluation is limited to uniaxial tensile tests [4]. The stress states applied to water pipes in service is multiaxial because of sudden impacts caused by earthquake, for example. Therefore, the uniaxial tensile test alone is not sufficient as a test method for evaluating the deformation characteristics of water pipe materials, and it is essential to elucidate the material characteristics under multiaxial stress states.

In this study, the deformation behavior of a HI-PVC tubular material was measured using the multiaxial tube expansion testing machine [5]. Moreover, a proper material model for reproducing both the work hardening behavior and the directions of the plastic strain rates under biaxial stress states was determined with good accuracy.

Experimental Methods

Fig. 1 shows the outline of the multiaxial tube expansion test method (MTET) used in this study. The MTET is a material test method, in which an arbitrary biaxial stress state is generated in the central part of the test piece by applying and feedback controlling the axial force and internal pressure [7]. A load cell and a water pressure gauge were used to measure the axial force and internal pressure, respectively. The axial and circumferential strains, ε_ϕ and ε_θ, were measured with an area camera

and a laser displacement meter [5]. Hereinafter, the axial and circumferential directions of the test piece are denoted as ϕ and θ, respectively.

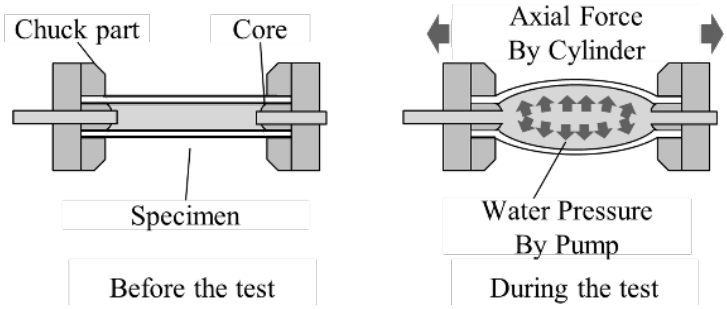

Fig. 1 Schematic diagram of the multiaxial tube expansion test.

The test material was HI-PVC water pipe produced by Kubota ChemiX Co., Ltd. with an outer diameter of 18 mm and an inner diameter of 13 mm. A circular HI-PVC tube with an initial length of 2 m was cut to a length of 110 mm for a test piece while it was cut to 120 mm for σ_ϕ: σ_θ= 0:1 to prevent contact between both cores inside the test piece.

Nine linear stress paths of σ_ϕ: σ_θ= 1:0, 4:1, 2:1, 4:3, 1:1, 3:4, 1:2, 1:4, and 0:1 were applied to the test pieces. The temperature during the test was 20.3 to 23.9 °C, and the loading speed was controlled so that the equivalent strain rate was almost constant at 1×10^{-3} $[s^{-1}]$.

Experimental Results

Fig. 2 (a) shows the variation of the measured equivalent strain rate with the increase of the equivalent strain for σ_ϕ: σ_θ =1:0, 1:1, and 0:1. We confirmed that the true stress increments were successfully controlled and applied to the specimens so that the von Mises equivalent plastic strain rate became roughly constant at 1×10^{-3} $[s^{-1}]$ for all stress paths.

The measured stress paths are shown in **Fig. 2 (b)**. We confirmed that the experimental stress paths well followed the referential ones for all nine paths. At σ_ϕ: σ_θ = 1:0, 4:1, 2:1, 4:3, 1:1, 3:4, and 1:2, we succeeded in measuring the forming limit stress (marked with a star mark). At σ_ϕ: σ_θ = 0:1 and 1:4, the bulge deformation of the test piece exceeded the allowable measuring range of the strain measurement apparatus.

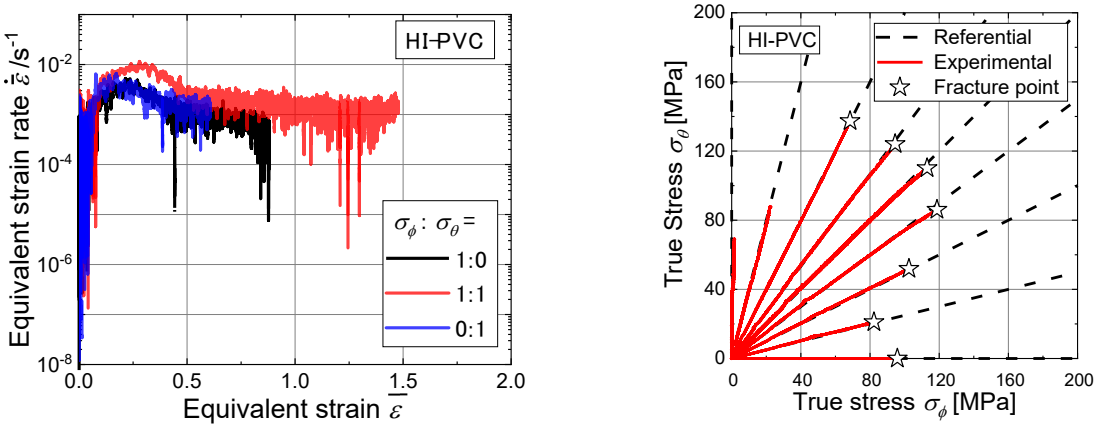

Fig. 2 (a) Variation of the measured equivalent strain rate with the increase of the equivalent strain and (b) reference and experimental stress paths of the multiaxial tube expansion tests.

From the true stress-logarithmic strain (ss) diagram in the low strain range at σ_ϕ: σ_θ = 1:0, a proportional relationship was confirmed between the stress and strain. Assuming this range as an elastic region, elastic strain was calculated associated with the true stress of the ss diagram, and the logarithmic plastic strain was obtained by subtracting the elastic strain from the total logarithmic strain. For other linear stress paths, the elastic slope was also identified within the range where the ss curve can be viewed as a straight line to calculate elastic strain. **Fig. 3** shows the logarithmic plastic strain paths ($\varepsilon_\phi^{\mathrm{p}}$, $\varepsilon_\theta^{\mathrm{p}}$) measured for each linear stress path. The strain paths for σ_ϕ: σ_θ =1:0, 4:1, and 4:3 are almost linear while those for σ_ϕ: σ_θ = 2:1, 1:1, 3:4, 2:1, 4:1, and 0:1 were nonlinear. For σ_ϕ: σ_θ=1:1, an equivalent strain of 1.47 was achieved, the largest of the nine stress paths.

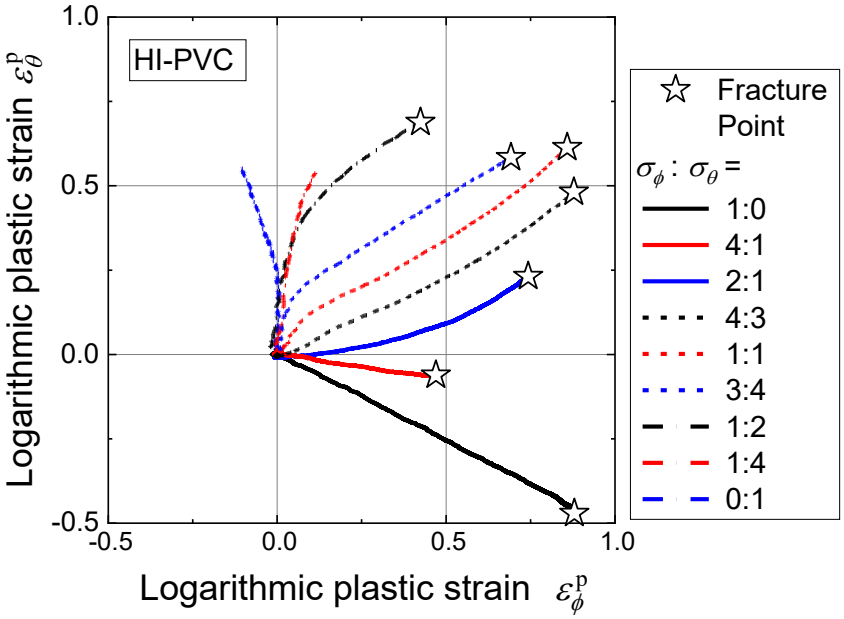

Fig. 3 Plastic strain paths measured for the linear stress paths.

Fig. 4 shows the direction of the plastic strain rate, β, measured for each stress path, which is represented by a loading angle, φ, in the stress space. β is 0 in the tube axis direction, and positive for the counterclockwise direction. For σ_ϕ: σ_θ=1:0, 4:1, 2:1, 4:3, 1:1, β is almost constant. While, for σ_ϕ: σ_θ = 3:4, 1:2, 1:4, and 0:1, β changes with the increase of $\varepsilon_0^{\mathrm{p}}$. For example, when φ = 90 °, β changes from 86° to 121°.

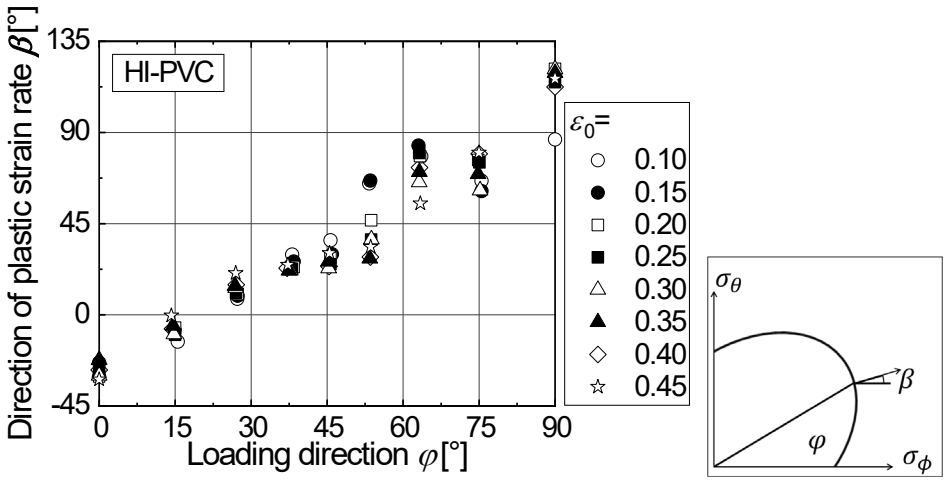

Fig. 4 Measured directions of plastic strain rates.

Contours of plastic work were created to quantitatively evaluate the work hardening characteristics of the test material subject to biaxial tensile stress. First, in the true stress-logarithmic plastic strain diagram of the uniaxial tensile test in the axial direction, the plastic work W_0 per unit volume consumed until the reference plastic strain of $\varepsilon_0^{\mathrm{p}}$ is calculated. Next, for other linear stress paths, the true stresses (σ_ϕ, σ_θ) at an instant when the same amount of plastic work as W_0 is consumed are plot on the principal stress space to determine contours of plastic work. In this study, we succeeded in measuring contours of plastic work up to $\varepsilon_0^{\mathrm{p}} = 0.45$ for all nine stress paths. **Fig. 5 (a)** shows the measured contours of plastic work. In addition, the stress values at every $\varepsilon_0^{\mathrm{p}}$ in Fig. 5(a) were normalized by σ_0 at σ_ϕ: σ_θ = 1:0. The normalized contours of plastic work are shown in **Fig. 5 (b)**. At σ_ϕ: σ_θ = 1:4 and 1:2, a significant expansion of the work contours was observed with the increase of $\varepsilon_0^{\mathrm{p}}$; the test sample exhibited anisotropic hardening.

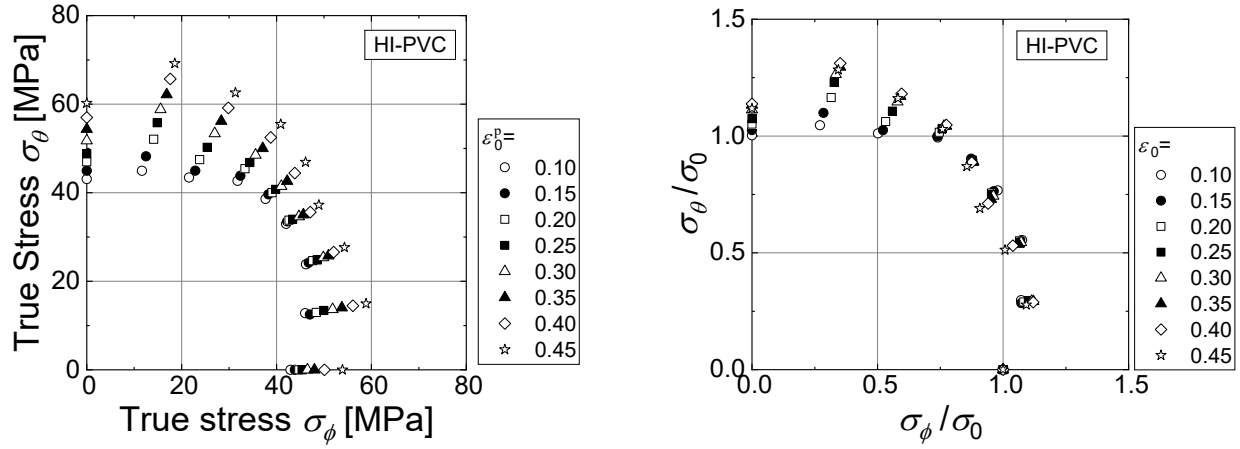

(a) (b)

Fig. 5 The results of the MTET. (a) Measured stress points forming contours of plastic work. (b) Contours of plastic work, normalized by the axial true stress, $\boldsymbol{\sigma_0}$, at $\boldsymbol{\sigma_\phi}$: $\boldsymbol{\sigma_\theta}$ = 1:0, belonging to respective work contours.

Material Modeling

Fig. 6 compares the measured work contour at $\varepsilon_0^{\mathrm{p}} = 0.45$ with the yield loci calculated using the von Mises yield function, Hill's quadratic yield function, and the Yld2000-2d yield function [6, 7]. The parameters of Hill's quadratic and the Yld2000-2d yield function were determined using yield stresses. The number of the parameters to be determined for Hill's quadratic yield function is three:

$$\left(A\sigma_x^2 - B\sigma_x\sigma_y + C\sigma_y^2\right)^{\frac{1}{2}} = 1. \tag{1}$$

The genetic algorithm method (GA method) was used to determine the exponent M and the six coefficients α_i(i=1~6) of the Yld2000-2d yield function so that the evaluation function f shown below was minimized [7]:

$$f = \sum_{i=1}^{N} w_{\sigma,i}(\delta' - \delta)^2 + \sum_{i=1}^{N} w_{\beta,i}(\beta' - \beta)^2 . \tag{2}$$

Here, N (=9) is the number of stress points forming a work contour, δ' is the distance between the origin of the principal stress space and the calculated yield locus along the stress path to the i-th stress point, δ is the distance between the origin of the principal stress space and the i-th stress point, β' is the direction of the plastic strain rate calculated using the yield function and the associated flow rule for the i-th stress path and β is the direction of the plastic strain rate measured for the i-th stress path. $w_{\sigma,i}$ and $w_{\beta,i}$ are weighting coefficients for each stress path, and it is possible to arbitrarily select the experimental values to be reproduced by changing the coefficients.

The von Mises yield function overestimates the stresses at σ_ϕ: σ_θ = 4:1, 2:1, 4:3, 1:1, and 3:4. Hill's quadratic yield function reproduces the tendency of the experimental data at σ_ϕ: σ_θ= 1:0, 4:1, 2:1, 4:3, and 1:1, but underestimated the stresses at σ_ϕ: σ_θ=3:4, 1:2, and 1:4. The yield loci calculated using the Yld2000-2d yield function is consistent with the measured work contour.

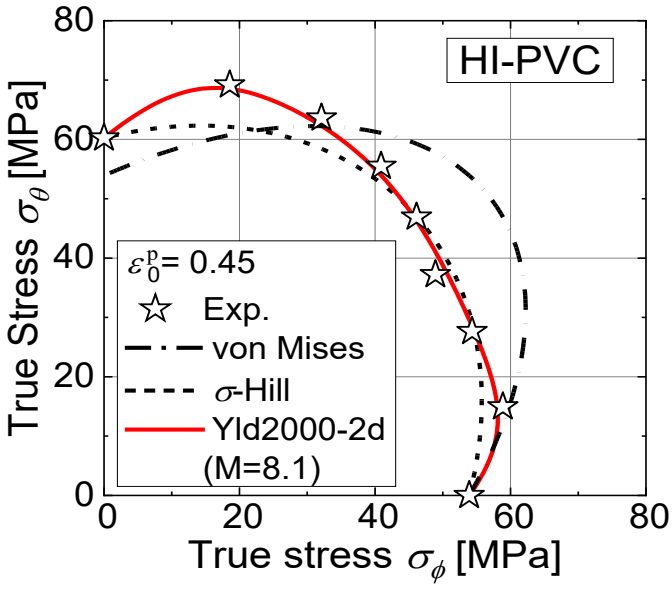

Fig. 6 Measured stress points forming contours of plastic work, compared with the yield loci calculated using selected yield functions.

Fig. 7 compares the directions of the plastic strain rates measured at $\varepsilon_0^p = 0.45$ with those predicted by the von Mises, Hill's quadratic, and the Yld2000-2d yield functions. **Fig. 8** shows the mean squared error, β_{MSE}, between the predicted and experimental data of the plastic strain rate. β_{MSE} was calculated using the following equation:

$$\beta_{MSE} = \frac{1}{N}\sum_{i=1}^{N}\left(\beta_{M,i} - \beta_{C,i}\right)^2. \tag{3}$$

where $\beta_{M,i}$ are the experimental values, $\beta_{C,i}$ are those calculated using the selected yield functions, and N is the number of the experimental data.

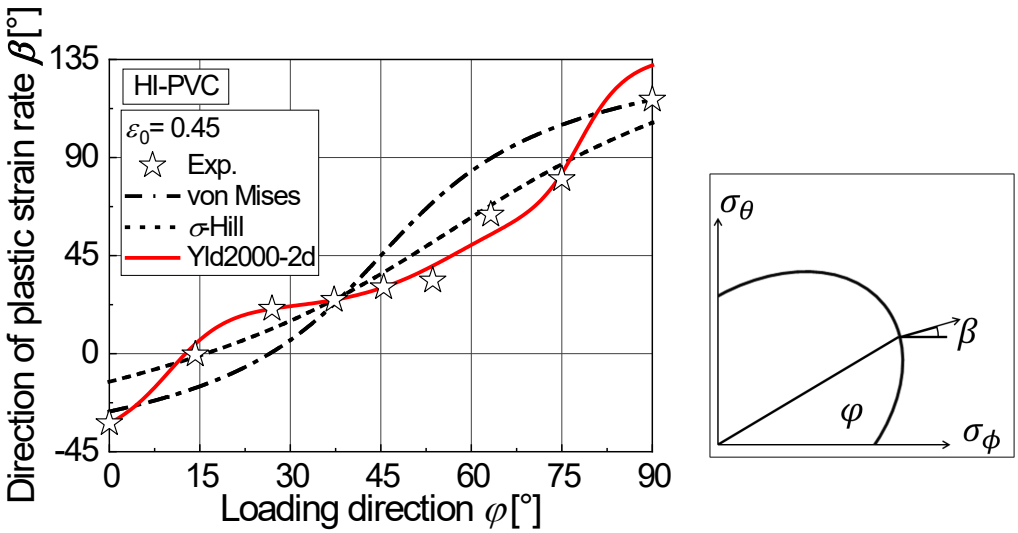

Fig. 7 Directions of the plastic strain rates and those calculated using selected yield functions.

The von Mises yield function has a large deviation from the experimental value, and the mean squared error is also the largest. Hill's quadratic yield function has a smaller error than the von Mises yield function, but it significantly deviates from the experiment at σ_ϕ: σ_θ= 1:0, 2:1, 1:1, 3:4, and 0:1. The Yld2000-2d yield function well reproduces the tendency of the experiment; the mean squared error is $\beta_{\mathrm{MSE}} = 0.01$, which is the smallest. From the results of Figs. 6 to 8, it is concluded that the Yld2000-2d yield function with $M = 8.1$ is the most appropriate material model for the test material, at least for the linear stress paths. It is noted that the work contour can be practically viewed as a plastic potential.

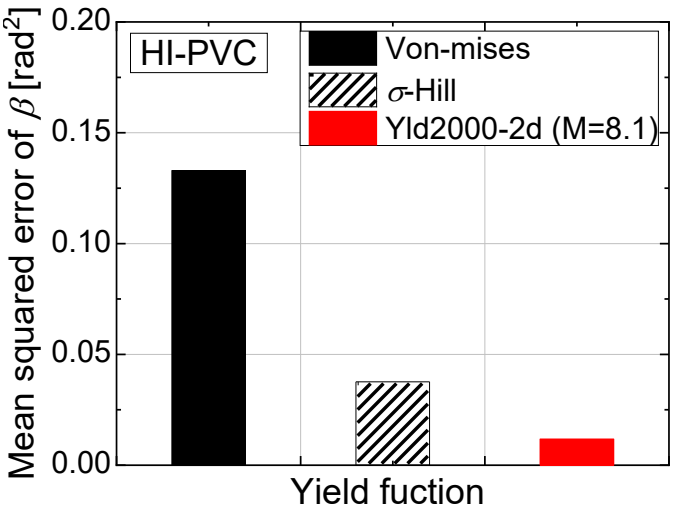

Fig. 8 Mean squared error of $\boldsymbol{\beta}$ evaluated for the selected yield functions.

As is shown in Fig. 5, the shapes of the work contours change with increasing $\varepsilon_0^{\mathrm{p}}$, or equivalently W_0. The differential hardening behavior of the test sample can be formulated by changing the parameters of the Yld2000-2d yield function as a function of W_0. Applying the created material model to FEA leads to an improvement in the accuracy of deformation analysis of the material. That will be the objective of the future work.

Conclusions

Nine linear stress paths were applied to the HI-PVC circular tube test piece using the MTET, and the deformation behavior was measured in detail. The following findings were obtained.

(1) We succeeded in measuring the forming limit strain and forming limit stress at σ_ϕ: σ_θ= 4:1, 2:1, 4:3, 1:1, 3:4, 1:2.

(2) True stress-logarithmic plastic strain curves were measured for all nine linear stress paths. In addition, the contours of plastic work were successfully determined up to reference plastic strain of $\varepsilon_0^{\mathrm{p}} = 0.45$. The test sample exhibited significant anisotropic hardening.

(3) The von Mises yield function, Hill's quadratic yield function, and the Yld2000-2d yield function were identified for the contour of plastic work at $\varepsilon_0^{\mathrm{p}} = 0.45$. The Yld2000-2d yield function had a better agreement with the measued work contour than Hill's quadratic and the von Mises yield functons.

(4) The test sample follows the normality rule with the Yld2000-2d yield function, at least for $\varepsilon_0^{\mathrm{p}} = 0.45$.

References

[1] T. Kuriyama, I. Narisawa, The effect of precracking techniques on fracture toughness of polymer, J. JSPP 1 (1989) 529-537.

[2] T. Makino, The environment and polymetric materials － II: Poly (Vinyl Chloride) and Environmental Issues, J. SMS 54 (2005) 221-227.

[3] Y. Ishiwatari, T. Kato, et al., Investigation of underwater camera images and suspended solid composition in lined water pipes and polyvinyl chloride pipes, J. JSWE 39 (2016) 43-50.

[4] H. Iizuka, T. Kunii, et al., Mechanical properties of a plastic-rubber composite material, J. SRST 71 (2001) 29-34.

[5] S. Kubo, T. Kuwabara, et al., Measurement and analysis of deformation behavior of polyethylene tube subjected to biaxial tensile stress with large strain, J. JSTP 62 (2021) 73-78.

[6] F. Barlat, J.C. Brem, J.W. J.W. Yoon, et al., Plane stress yield function for aluminum alloy sheets － part 1: theory, Int. J. Plast. 19 (2003) 1297−1319.

[7] T. Hakoyama, T. Kuwabara, Effect of biaxial work hardening modeling for sheet metals on the accuracy of forming limit analyses using the Marciniak-Kuczynski approach, in: H. Altenbach, T. Matsuda, D. Okumura (Eds.), From Creep Damage Mechanics to Homogenization Methods, Springer, Heidelbeg, 2015, pp. 67-95.